Engineering and Technology Journal e-ISSN: 2456-3358
Volume 07 Issue 10 November-2022, Page No.-1680-1689
DOI: 10.47191/etj/v7i11.06, I.F. – 6.484

Evaluation of the Bottom Surface Water Jet Impingement Cooling Rate Using Modified Run-Out Table

A. M. Nwankwo[1], E. A. Chinachi[2], I. C.C. Iloabachie
[1,2]Department of Mechanical Engineering, Caritas University Amorji-Nike Enugu Nigeria
[3]Department of Mechanical, Institute of Management and Technology, Enugu, Nigeria.

ABSTRACT: Evaluation of Temperature-Time Profiles by the Lumped Thermal Mass analysis method for bottom surface jet impingement cooling system was carried out. This was done by controlled accelerated cooling using a modified run-out table (ROT). The evaluation was with variant pipe diameters of 10mm - 40mm by a single water jet, having impingement gaps in the range of 55mm - 95mm and controlled sub-cooled to a range of 150ºC – 110ºC. The results revealed that the cooling rate was faster at an impingement gap of 95mm in all the pipe diameters. This was evident from the plot of temperature-time, with a gap of 95mm showing 1.93ºC/s and 3.24ºC/s at diameters of 10mm and 40mm respectively. This evidently revealed that at any given pipe diameter the cooling rate is higher at a higher impingement gap for bottom surface-controlled cooling. This is also suggested by the calculated heat transfer coefficient that shows an increase with the increase in pipe diameter and impingement gap for an increase in cooling rate. Therefore, for bottom surface jet impingement cooling, a higher impingement gap for any pipe diameter will give a better cooling rate for the steel austempering process.

KEYWORDS: Modified Run-out table, Cooling rate, bottom surface, impingement gaps, controlled accelerated cooling, lumped thermal mass analysis

INTRODUCTION

Recently, with the continual enhancement of steel material functions, such as higher strength and better ductility, the growing demand for cost-cutting by reducing the use of alloying elements and streamlining processes: the thermo-mechanical control process (TMCP) has become increasingly important (Kazuaki et al, 2016). Steel and other alloys have a huge number of applications in engineering practice under very many conditions, requiring that the steel will have several properties for various applications (Alqash, 2015). At one point of the designer's desired need, steel materials are subject to either of the following: bending and at the other to twisting. As tool materials that will cut others, they may be requiring hardness and toughness with no brittle cutting edge and they may as well be able to withstand various kinds of stresses. Also, they may be applied in an area where they will require by designers at various times to bear static and dynamic loads, rotates at very low or high speed, carry extreme hard skin with a tough core, work under very high corrosive area, and subject to creep, fatigue, and impact, etc. Serving under these conditions, they require certain specific properties to be able to successfully withstand the various condition the designers subject them to (Antonio et al, 2014). Meanwhile, some materials may fully or partially be lacking in these specifics. These lacks or deficiencies are fulfilled before now through the process of heat treatment, which is not cost-effective and does not give designers their needs at all times. Therefore, there is a need for improving steel properties, which demand reducing the cost of alloying elements, and streamlining processes, Hence, need for a better process in steel production that tells heating and control cooling (Kazuaki et al, 2016). In particular, the hot-rolling process, which is a well-known manufacturing method of steel strips, requires great management since it has a crucial influence on the properties of the final product (Alqash, 2015) The improved design ROT by (Onah, 2018) was for top surface stationary only, bottom surface reticulation was lacking, and we have bottom surface reticulation done. Mechanistic modeling of pool boiling has been in existence and it is cumbersome to analyze, hence the need for a simpler model of analysis – lumped thermal mass analysis. Hence, evaluation of temperature-time profile by lumped thermal mass using a bottom surface cooling system of jet impingement on the modified run-out table.

(Noel, 2006) Studied the cooling system of boiling heat transfer on a hot steel plate cooled by an inclined circular bottom surface water jet. He focused on the inclined angle at the bottom of the steel hot plate, and the flow rate effect on heat extraction. He varied the flow rate, ROT speed, and inclined angles from 35 -55l/min, 0 -1 m/s, and 10-30ºC respectively. With these variables, he employed the inverse heat conduction model and his measurements and calculated the boiling curve or heat fluxes as a function of plate surface temperature.

In the work carried out by (Jeffery, 2011), using a downward facing plate–bottom surface cooling process, he explained, that in a free-surface impingement type of cooling, upon impingement to the surface, the direction of the liquid change to a diagonal along the plate shown in schematics of Fig. 1 below, the surface produce evaporation and boiling. Nozzle-to-surface spacing (H_n) can influence the velocity and size of the jet before impinging on the surface,

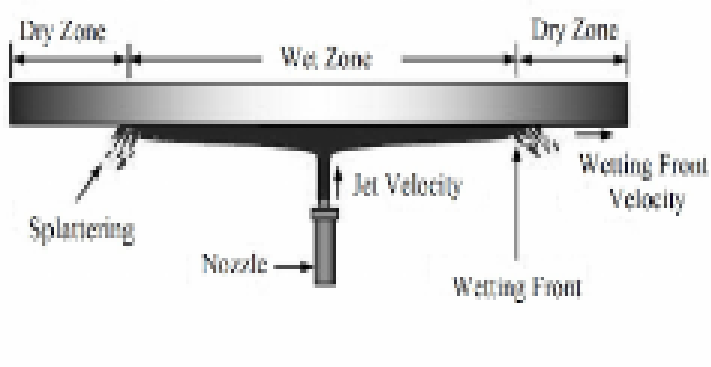

Figure 1. Schematics free surface bottom impingement jet cooling model (Molana et al, 2013)

(Mitsutakee et al, 2001) Carried out an experiment on a transient heat transfer by boiling with single bottom water jet impingement cooling upward on a hot cylindrical copper block. The heat was supplied to 250ºC, the parameters were still 2mm diameter nozzle, subcooling temperature 20 – 80k jet velocity of 5 -15m/s. Using a two-dimensional heat conduction wall, heat flux evaluation at different depths using a numerical model was done. Their results showed that the regime of nucleate boiling seems to occur where the wetting front is, which is where the max heat fluxes occur.

(Roy, 2011), they experimented with quenching stainless steel using a single jet oil impingement cooling process on the bottom surface of the plate. They heated the sample specimen from 100ºC to 900ºC and their objective was to know the effect of oil as an impingement fluid on the bottom surface. Their varying parameters were 113 to 381ml/min, oil pressure 3.1 to 12 psi, and impingement height of 0.6 to 1 cm. Test results also show that oil heat transfer coefficient and heat flux keep increasing as plate temperature increases. Comparing the boiling curves for oil to water, the boiling curve for oil shifts to a higher temperature range where the peak in heat transfer can be expected to occur at a temperature much higher than that required for water. Also, nozzle-to-plate distance has affected heat transfer.

1.1. Experimental Test Facility and Procedure Test Facility

The Improved design of the run-out table analyzed and modeled by a mechanistic pool boiling mechanism (Onah, 2018) lacked a bottom surface cooling system. As shown in fig. 2. This study handled multiple jet impingement-controlled cooling.

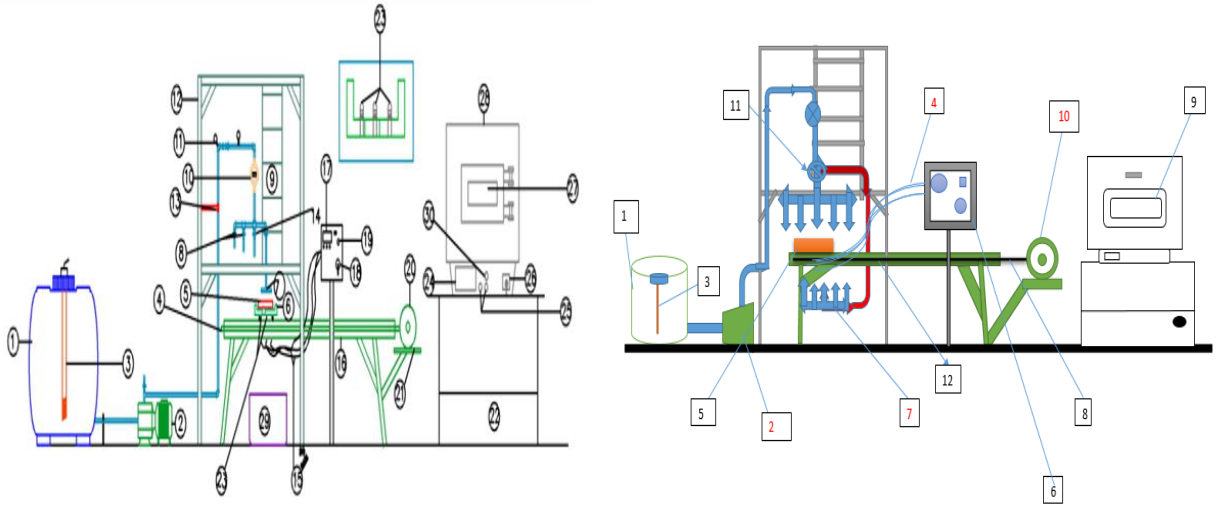

Figure 2. Schematic diagram of ROT (L) The Improved Design plant (Onah, 2018) **(R) Modified Design.**

The modified design consists of 1. Water tank, 2. Electric pump, 3.Heater, 4. Thermocouple wires, 5.The workpiece and its carrier, 6.Thermocouple control panel, Workpiece bed, 7. Bottom surface Impingement nozzle headers, 8. Motorized screw conveyor, 9. Furnace, 10. Electric motor,

11. Flow valve, 12. Flow meter, 13. Ladder, 14. Furnace support, 15, PVC Pipes, 16. Pressure gauge, 17.

MATERIALS AND METHOD

Fig. 3 shows a schematic diagram of a pilot modified scale run-out table (ROT) facility modified for bottom surface cooling, installed at Metallurgical and Material Engineering Laboratory (MMEL), ESUT. The modification involves the installation of bottom reticulation PVC pipes for the bottom process and installation of a flow meter etc.

Using a guide attached to the Asynchronize Rotor gear powered conveyor drive system of 0.75kw of 1500rpm, operating at a ratio of 1:24 with 50Hz on an AC of 240volts, the sample was driven to the cooling header for the experiment. The experiment features the cooling system – a closed loop where the volume of water used was 1.56m^{3,} circulated throughout the system. Initial temperature, water temperature, impingement height, and flow rate were varied and controlled at variant pipe diameters. DAB water pump of 25m head, with 58L/min flow rate, was employed. It pumped water to the sampled plate from the water tank below to the target plate through the flow meter, and nozzle header via the impingement jet nozzle to the hot plate. An electric heater of 9kw of 330volts was situated in the tank and was to adjust the temperature of water between 10-50oC. The water temperature readings were taken by mercury in a bulb thermometer. Attached four thermocouples were read out using the mounted control panel for the temperature and average taken.

Controlled volume of lumped Thermal Mass Model Analysis for Convective Heat Transfer Co-efficient h Evaluation

Before now pool boiling mechanism has been the main model for predicting impingement heat transfer. This model is very cumbersome and wastes a lot of time, which gives a contestable error margin. Hence, the employment of lumped thermal mass model can be validated using the Biot dimensionless number. The basic concept in the analysis of the lumped thermal mass model; is that the interior temperature of the body remains constant at all times during a heat transfer process. The temperature of such a body is only a function of time, $T = T(t)$. This also means that in analysis, no temperature gradient exists -which means that the body's internal resistance (conduction) is negligible compared to total resistance (convection). In this model, when a mass, a well-conducting solid or a well-mixed fluid, is subjected to heating or cooling by exposure to an environment with which it exchanges heat, one assumes that temperature variations within the mass can be neglected in comparison with the temperature difference between mass and the surrounding fluids. (Shankar, 2019).

The control volume of the lumped thermal mass model of the impingement process in Fig. 4 simplifies the complicated modeling process of impingement cooling which involves conduction and convection. In this process, we assumed that:

i. Heat transfer from a hot steel plate is seen as a lumped mass.
ii. The mass resistance heat transfer is negligible when compared with resistant heat transfer with the impinging fluid.
iii. The volume of the mass remains unchanged.

The 2-D Bottom and top surface cooling heat transfer deal with a thickness of 12mm and length of 230mm with a width of 120mm.

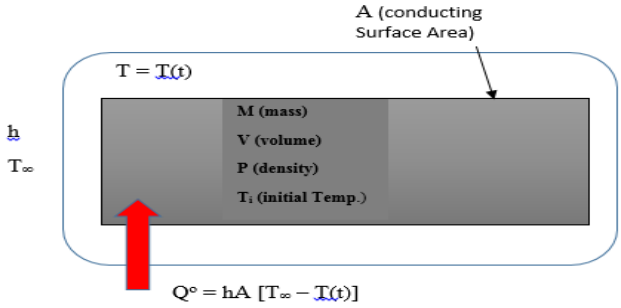

Figure 3. Control volume of the lumped thermal mass model Analysis of impingement process

By the lumped mass method based on the control volume of steel plate Fig. 4, mass behaves as a single lump of temperature, T. Thus equating heat transfer conduction at the bottom to that conducted at the top by convection, since boiling heat is infinitesimal and was collapsed into convection, in equation (1) as;

$$MC\frac{d}{dt}(T_S - T_\infty) = -hA(T_S - T_\infty) \qquad (1)$$

$$\frac{\partial(T_s - T_\infty)}{(T_s - T_\infty)} = \frac{-hAdt}{mcp} \qquad (2)$$

By integration,

$$\int_{t=0}^{t} \frac{d(T - T_\infty)}{T - T_\infty} = Log_e\left(\frac{T - T_\infty}{T_S - T_\infty}\right) t = 0, = \frac{-hAt}{mcp} \qquad (3)$$

Thus, $Log_\theta = \frac{-hAt}{mcp}$ (4)

The gradient is given as in equation 6, as,

$$\text{gradient is } -\propto = \frac{-hAt}{mcp} \quad (5)$$

From which, $h = \propto \rho wcp$ (6)

Where h is convective heat transfer coefficient W/m^{2}k

$for\ steel, density\ \rho = \frac{7900hg}{m^3}$, $specific\ heat\ Cp = \frac{500J}{kgk}$; $sampled\ thickness\ w = 0.012m$, $\propto$, is the gradient from equation (5)

RESULTS AND DISCUSSION

Evaluating temperature-time of the Bottom surface stationary cooling process of constant impingement diameters, varying impingement gaps at a controlled Cooled Temperature of 150ºC@ Diameter D= 10mm, Results of experimental temperature-time are presented in Tables 1 – 5 which were used to obtain temperature-time plots of Figs 5 - 9, for the controlled cooling temperatures of 150ºC, 140ºC, 130ºC, 120ºC, 110ºC at constant impingement diameters of D= 10mm, 15mm, 30mm, 35mm, 40mm respectively that corresponds to initial surface temperatures 450ºC, 440ºC, 430ºC, 420ºC and 410oC, also corresponding to different impingement gaps of 55mm, 65mm, 75mm, 85mm and 95mm respectively.

Table 1 shows the various surface temperatures and Times at variant impingement gaps for a diameter of 10mm sub-cooled to 150ºC.

Table 1. Temperature and Time at 150ºC for D=10mm Variant T and H

T=450 @D=10mm(H=55)		T=440 @D=10mm(H=65)		T=430 @D=10mm(H=75)		T=420 @D=10mm(H=85)		T=410 @D=10mm(H=95)	
T(s)	**Ts**	**T(s)**	**Ts**	**T(s)**	**Ts**	**T(s)**	**Ts**	**T(s)**	**Ts**
0	450	0	440	0	430	0	420	0	410
64	400	55.2	361.67	53.6	383.34	50.3	375	48.15	366.67
128	350	110.4	343.33	107.2	336.68	100.6	330	96.3	323.34
192	300	165.6	295.01	160.8	290.02	150.73	285	144.45	280.01
256	250	220.8	246.68	214.4	243.36	201.03	240	192.6	236.68
320	200	276.6	198.35	268	196.7	251.33	195	240.75	193.35
384	150	331.2	150	321.6	150	301.63	150	288.9	150

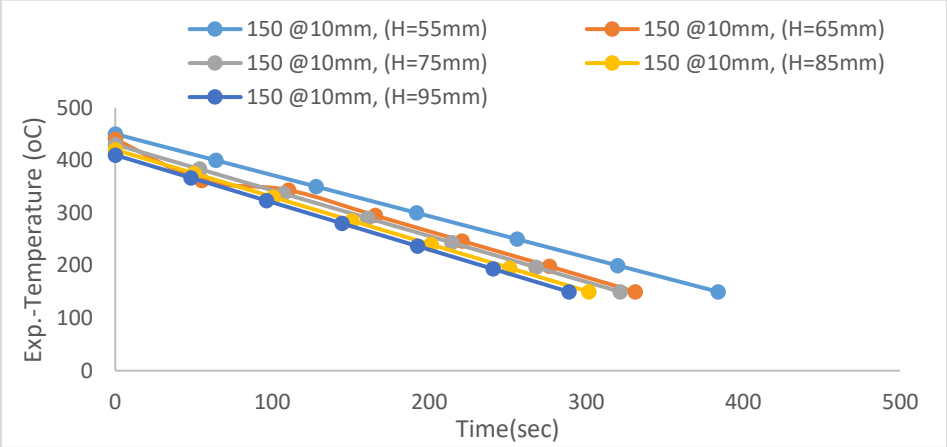

Figure 4. Temperature-time Controlled Cooling Profile @ 150ºC for D=10mm with variant H

Fig. 5: is the temperature-time controlled cooling profile for a diameter of 10mm and varied impingement gaps. From the downward linearity of the plot, the cooling rate was highest at H= 95mm with 1.93ºC/s. Also, H= 85mm followed with 2.01ºC/s, H= 75mm with 2.14ºC/s, H= 65mm has 2.21ºC/s and H= 55mm with 2.56ºC/s.

Table 2 shows the various surface temperatures and Times at variant impingement gaps for a diameter of 15mm sub-cooled to 140ºC.

Table 2. Temperature and Time at 140ºC for D=15mm Variant T and H

T=450 @D=15mm(H=55)		T=440 @D=15mm(H=65)		T=430 @D=15mm(H=75)		T=420 @D=15mm(H=85)		T=410 @D=15mm(H=95)	
T(s)	**Ts**	**T(s)**	**Ts**	**T(s)**	**Ts**	**T(s)**	**Ts**	**T(s)**	**Ts**
0	450	0	440	0	430	0	420	0	410
63.1	398.34	61	390	58.4	381.67	53.3	373.34	51.3	365

126.2	346.68	122	340	116.8	333.34	106.6	326.68	102.6	320
189.3	295.02	183	290	175.2	285.01	159.9	281.68	153.9	275
252.4	243.36	244	240	233.6	236.68	213.2	235.02	205.2	230
315.5	191.7	305	190	292	188.35	266.5	188.36	256.5	185
378.6	140	366	140	350	140	319.8	140	307.8	130

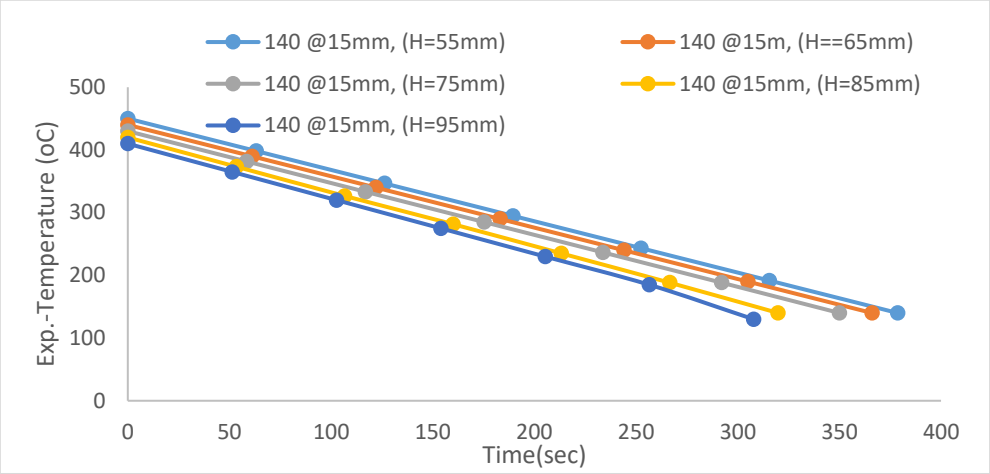

Figure 5. Temperature-time Controlled Cooling Profile @ 140°C for D=15mm with variant H

Fig. 6 is the temperature-time controlled cooling profile for a diameter of 15mm and varied impingement gaps. From the downward linearity of the plot, the cooling rate was highest at H= 95mm with 2.19°C/s. However, H= 85mm followed with 2.28°C/s, H= 75mm with 2.33°C/s, H= 65mm has 2.61°C/s and H= 55mm with 2.70°C/s.

Table 3 shows the various surface temperatures and Times at variant impingement gaps for the diameter of 30mm sub-cooled to 130°C.

Table 3. Temperature and Time at 130°C for D=30mm Variant T and H

T=450 @D=30mm(H=55)		**T=440 @D=30mm(H=65)**		**T=430 @D=30mm(H=75)**		**T=420 @D=30mm(H=85)**		**T=410 @D=30mm(H=95)**	
T(s)	**Ts**	**T(s)**	**Ts**	**T(s)**	**Ts**	**T(s)**	**Ts**	**T(s)**	**Ts**
0	450	0	440	0	430	0	420	0	410
62.54	396.67	59.44	388.34	57.64	380	55.06	371.67	53.2	363.34
125.08	343.37	118.8	336.68	152.28	330	110.12	323.34	106.4	316.68
187.62	290.07	178.32	285.02	172.92	280	165.18	275.01	159.6	270.02
250.16	236.74	237.76	233.36	230.56	230	220.24	226.68	212.8	223.36
312.7	183.41	297.2	181.7	288.2	180	275.3	178.35	266	176.7
375.24	130	356.64	130	354.84	130	330.36	130	319.2	130

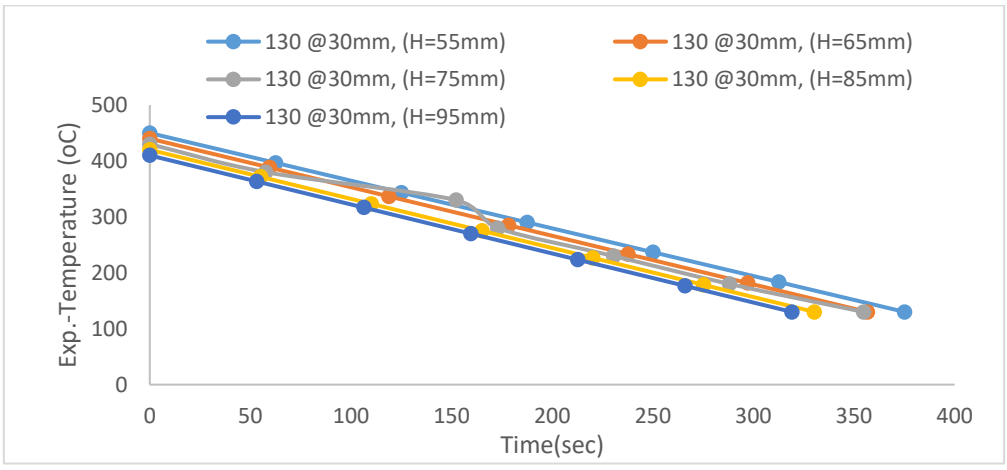

Figure 6. Temperature-time Controlled Cooling Profile @ 130°C for D=30mm with variant H

Fig. 7 is the temperature-time controlled cooling profile for a diameter of 30mm and varied impingement gaps. From the downward linearity of the plot again it continued the same drift, cooling rate wathe s highest at H= 95mm with 2.46°C/s. And H= 85mm followed with 2.54°C/s, H= 75mm with 2.73°C/s, H= 65mm has 2.74°C/s and H= 55mm with 2.89°C/s.

Table 4 shows the various surface temperatures and Times at variant impingement gaps for a diameter of 35mm sub-cooled to 120°C.

Table 4. Temperature and Time at 120°C for D=35mm Variant T and H

T=450 @D=35mm(H=55)		T=440 @D=35mm(H=65)		T=430 @D=35mm(H=75)		T=420 @D=35mm(H=85)		T=410 @D=35mm(H=95)	
T(s)	Ts	T(s)	Ts	T(s)	Ts	T(s)	Ts	T(s)	Ts
0	450	0	440	0	430	0	420	0	410
63.33	395	61.22	386.67	59.7	378.34	57.44	370	55.13	361.67
126.66	340	122.44	333.34	119.4	326.68	114.88	320	110.26	313.34
189.99	285	183.66	280.01	179.1	275.02	172.32	270	165.39	265.01
253.32	230	244.88	226.68	238.8	223.36	229.76	220	220.52	216.68
316.65	175	306.21	173.35	298.5	171.76	287.2	170	275.65	168.35
379.98	120	367.54	120	358.2	120	344.64	120	330.78	120

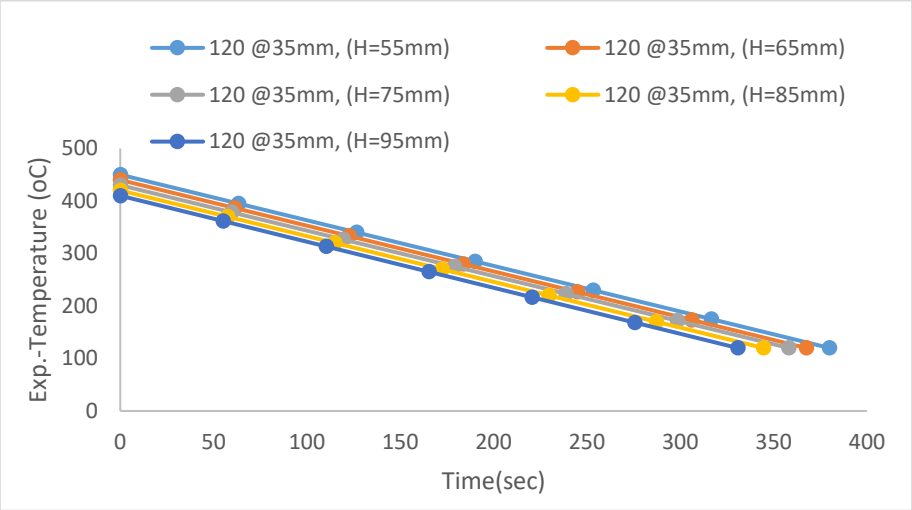

Figure 7. Temperature-time Controlled Cooling Profile @ 120°C for D=35mm with variant H

Fig. 8 is the temperature-time controlled cooling profile for a diameter of 35mm and varied impingement gaps. From the downward linearity of the plot again it sustained the same trend, the cooling rate was highest at H= 95mm with 2.76°C/s. Besides, H= 85mm followed with 2.87°C/s, H= 75mm with 2.99°C/s, H= 65mm has 3.06°C/s and H= 55mm with 3.17°C/s.

Table 5 shows the various surface temperatures and Times at variant impingement gaps for diameter 40mm sub-cooled to 110°C

Table 5. Temperature and Time at 110°C for D=40mm Variant T and H

T=450 @D=40mm(H=55)		T=440 @D=40mm(H=65)		T=430 @D=40mm(H=75)		T=420 @D=40mm(H=85)		T=410 @D=40mm(H=95)	
T(s)	Ts	T(s)	Ts	T(s)	Ts	T(s)	Ts	T(s)	Ts
0	450	0	440	0	430	0	420	0	410
66.06	393.34	64.43	385	65	376.67	60.02	368.34	59.4	360
132.12	336.68	128.86	330	130	323.34	120.04	316.68	118.8	310
198.18	280.02	193.29	275	195	279.01	180.06	265.02	178.2	260
264.24	223.36	257.72	220	260	216.68	240.08	213.36	237.6	210
330.3	166.7	322.15	165	325	163.35	300.1	161.7	297	160
396.36	110	386.58	110	390	110	360.12	110	356.4	110

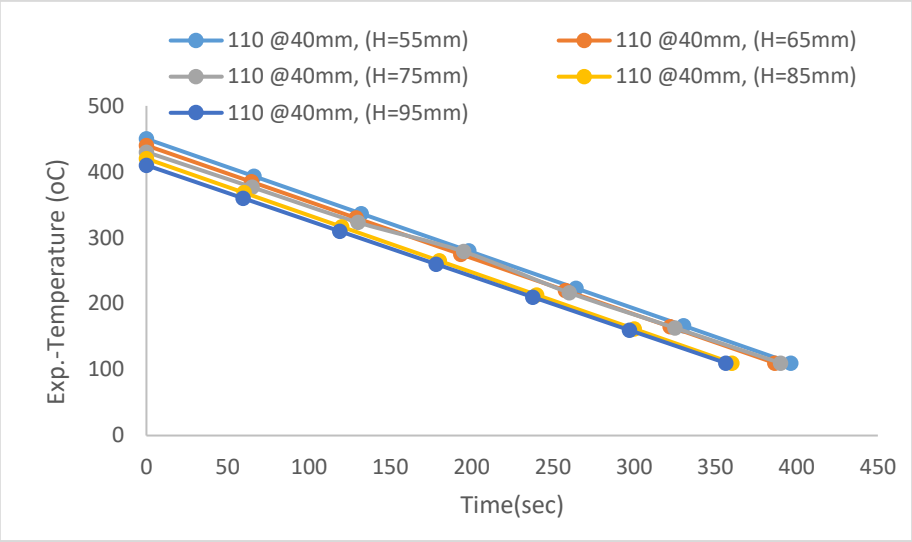

Figure 8. Temperature-time Controlled Cooling Profile @ 110ºC for D= 40mm with variant H

Fig. 9 is the temperature-time controlled cooling profile for a diameter of 40mm and varied impingement of the gaps. From the downward linearity of the plot again it maintained the same trend, the cooling rate was highest at H= 95mm with 3.24ºC/s. It revealed that heat extraction rate is higher impingement gap H. While H= 85mm followed with 3.60ºC/s, H= 75mm with 3.55ºC/s, H= 65mm has 3.51ºC/s and H= 55mm with 3.60ºC/s. Hence lower impingement gap rate of heat extraction is lower for bottom surface-controlled cooling.

This generally deduced that cooling rate for bottom surface-controlled cooling smaller pipe diameter with longer impingement gap will extract heat faster in an austempering of hot rolled steel for better mechanical and metallurgical properties of steel grades.

Evaluated Convective Heat Transfer Coefficients (h) from Lumped Thermal Mass Analysis

The results of the experiments for temperature-time were then further analyzed by lumped thermal mass analysis which showed the same linear decrease from various surface temperatures to various cooling times of the form $y = -\propto x + a$ for $R^2 = b$, where $\propto$ the slope used for estimation of various convective heat transfer co-efficient h values from Equation (5).

Ln (theta) Controlled at temperature 150ºC, Table 6 presented the ln (theta) temperature-time values used for generations of Figs 10 for the controlled temperature of 150ºC at a constant impingement diameter of D= 10mm, at the different impingement gaps. This was replicated for the other diameters at their variant impingement gaps and sub-cooled temperatures for the calculation of convective heat transfer coefficient h.

Table 6. Ln (theta) Temperature-Time for D= 10mm and 40mm Controlled @150ºC and 110ºC

WATER JET IMPINGEMENT COOLING (W-JIC) T= 450 @D = 10mm(H=55mm)					WATER JET IMPINGEMENT COOLING (W-JIC) T= 410^{0}C @ D = 40mm (H= 95mm)				
T_s	T_f	theta	T(s)	Ln (Theta)	T_s	T_f	theta	T(s)	Ln(Theta)
450	50	1	0	0	410	59	1	0	0
400	50	0.875	64	-0.13353	360	59	0.769821	59.4	-0.2615973
350	50	0.75	128	-0.28768	310	59	0.6419437	118.8	-0.4432546
300	50	0.625	192	-0.47	260	59	0.5140665	178.2	-0.6654027
250	50	0.5	256	-0.69315	210	59	0.3861893	237.6	-0.9514277
200	50	0.375	320	-0.980839	160	59	0.258312	297	-1.353587
150	50	0.25	384	-1.38629	110	59	0.1304348	356.4	-2.0368819

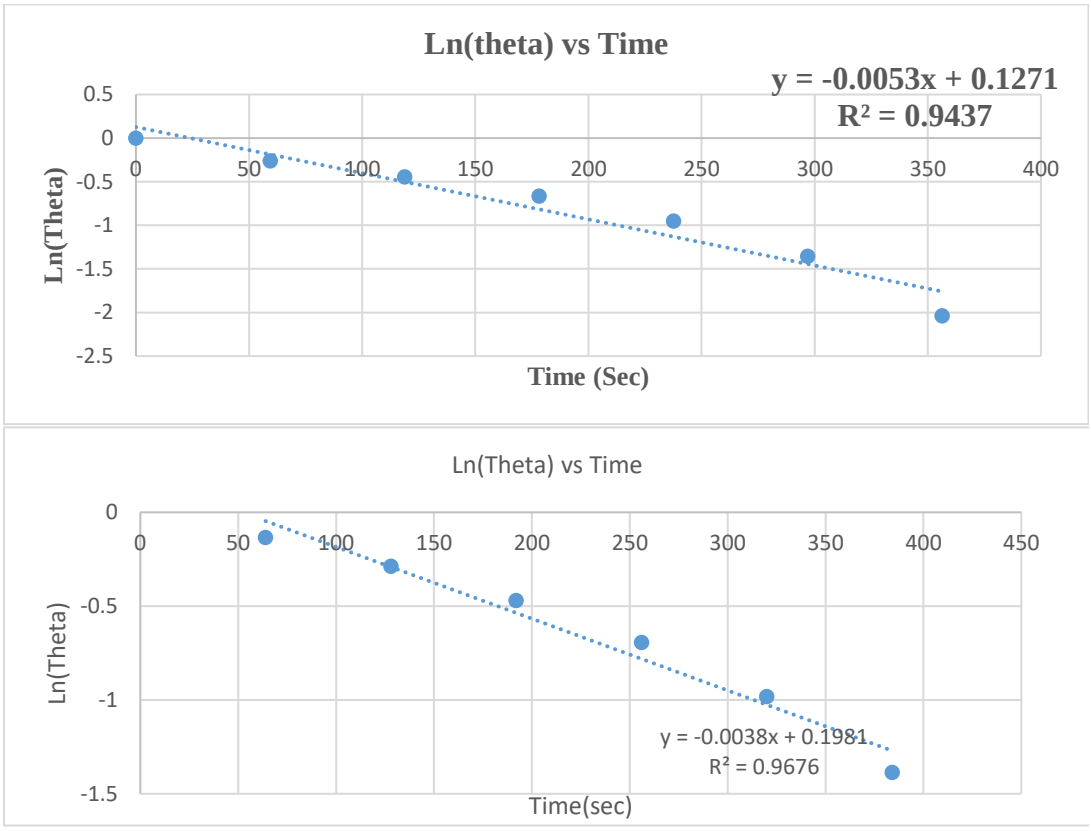

Figure 9. Ln(theta) Temperature-Time @150ºC and 110ºC for D=10mm and 40mm

The values of the slope of the lumped thermal mass analysis ∝, in ln(theta) temperature against time for determination coefficient of convective heat transfer (h), showed the same pattern of linear increase from constant impingement diameter of 10mm and varied impingement gap of 55mm, to 15mm diameter and varied impingement gap of 65mm. Also from 30mm diameter and varied impingement gap of 75mm to the diameter of 35mm and varied impingement gap of 85mm up to 40mm diameter and varied impingement gap of 95mm respectively, irrespective of the controlled temperature. This is suggestive that the various values of heat transfer coefficient (h) as obtained, would be more at a constant impingement diameter of 40mm and varied impingement gap of 95mm.

Calculated Heat Transfer Co-efficient h From Controlled Volume of Lumped Thermal Mass Analysis

Results of calculated values of heat transfer coefficient (h), from lumped mass analysis based on controlled volume Equation (5) at constant diameters D=10, 15, 30, 35, and 40mm with varying impingement gaps H=55mm, 65mm, 75mm, 85mm and 95mm, at a controlled temperatures 150ºC, 140ºC, 130ºC, 120ºC and 110ºC that corresponds are shown in Table 7.

Table 7. Calculated Heat Transfer Coefficient from Lumped Thermal Mass

H (mm)	Heat Transfer Coefficient h (w/m^{2}k)				
	D= 10mm	D= 15mm	D= 30mm	D= 35mm	D= 40mm
115	180.12	184.86	199.08	218.04	227.52
125	184.86	184.86	208.56	222.78	232.26
135	189.6	194.34	208.56	222.78	237
145	199.08	203.82	218.04	227.52	241.74
155	203.82	222.78	222.78	237	251.22

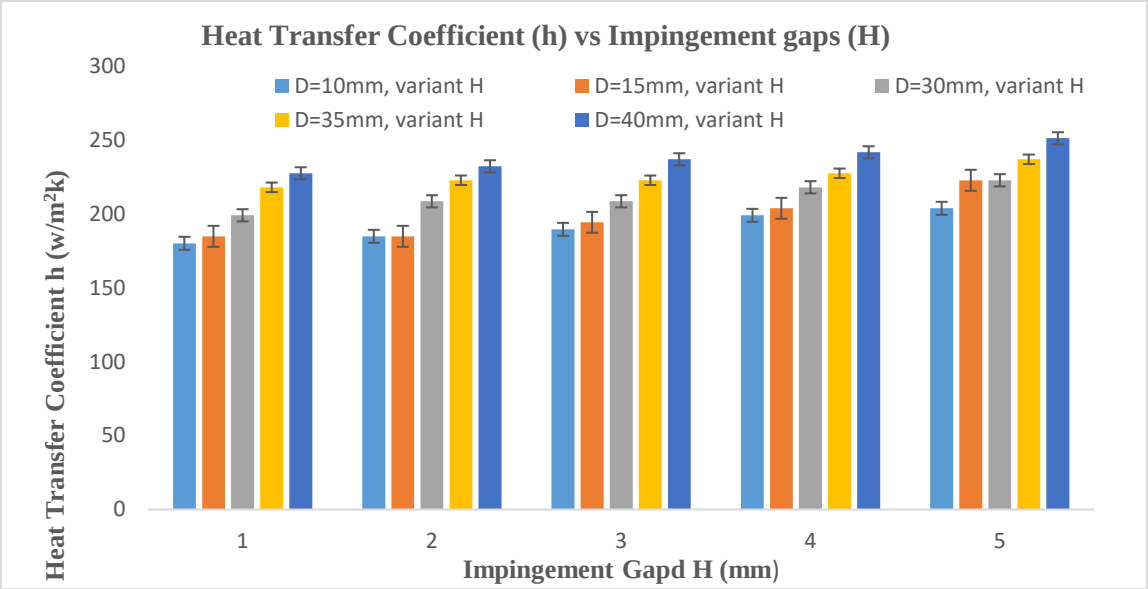

Figure 10. Effect of heat transfer coefficient h on impingement gaps and Diameters

Generally, it suggests that heat transfer coefficient (h) increases with an increase in pipe diameter (D) with a corresponding increase in impingement gaps (H)

This deduces that at any given constant pipe diameter(D), the flow rate (Q), decreases with a corresponding increase in impingement gap (H), resulting in increased heat transfer coefficient (h), where proficient higher heat extraction rate on hot-rolled steel plates cooling in steel mill industry. This would achieve better microstructures of steel at controlled temperatures in the heat transfer process.

CONCLUSION

The temperature-time profile of bottom surface cooling approximately showed the same cooling pattern the jet impingement parameters. From surface temperature range 450o°C to 410°C cooled linearly in the range of 150°C to 110°C by finite temperature profile across the sampled work-piece. The cooling rate at different pipe diameters shows that bottom surface cooling is best achieved at a higher impingement gap H. This was evident at a diameter of 10mm having 2.6°C/s at an impingement gap of 55mm against an impingement gap of 95mm with 1.9°C/s. Accordingly, the rest of the diameters maintained the same pattern of higher cooling rate with a lower impingement gap, with a diameter of 40mm having 3.2°C/s for an impingement gap of 95mm and 3.6°C/s for an impingement gap of 55mm. This is suggestive that the cooling rate for bottom surface controlled impingement cooling is better achieved at any pipe diameter with a lower impingement gap H. It was also observed that an increase in heat transfer coefficient increases the cooling rate.

AUTHOR CONTRIBUTION

All authors contributed equally to this work.

FUNDING

This research received no specific grant from any funding agency in the public, commercial, or not-for-profit sectors.

DATA AVAILABILITY STATEMENT

The data that support the findings of this study are available on request from the corresponding author.

CONFLICTS OF INTEREST

The authors declare that there are no conflicts of interest associated with this work

REFERENCES

1. Alqash, S. I. (2015). Numerical Simulations of Hydrodynamics of multiple water jets impinging over a horizontal moving plate. In *Numerical Simulations of Hydrodynamics of multiple water jet impinging over a horizontal moving plate* (p. 125). Vancouver: University of British Columbia, Vancouver.
2. Antonio et al. (2014). Accelerated Cooling of Steel Plates: The Time has Come. *Journal of ASTM International*, *5*, 8 - 15.
3. Jeffery, A. (2011). *Advanced Engineering Mathematics.* Academic Press.
4. Kazuaki et al. (2016). Water Quenching CFD (Computational Fluid Dynamics) Simulation with Cylindrical Impinging Jets. *NIPPON Stell and SUMITOMO Metal Technical Report, no III*, pp. 621 - 771. Osaka.
5. Mitsutakee et al. (2001). Heat Transfer During Transient Cooling of High-Temperature Surface with Impingement Jet. *International Journal of Heat and Mass Transfer*(37), 321 - 330.
6. Molana et al. (2013). Investigation of Heat Transfer Processes Involved Liquid Impingement Jets: A

Review. *Brazilian Journal of Chemical Engineering, 30*(03), 413-435.

7. Noel, L. C. (2006). *A Study of Boiling Heat Transfer on a Hot Steel Plate Cooled By Inclined Circular Bottom Water Jet; M.Sc. Thesis on Material Engineering.* The University of British Columbia.
8. Onah. (2018). Evaluation Temperature Profile on Pool Boiling Using Jet Impingement Cooling System. *American Journal of Engineering Research*, 304-310.
9. Onah T. O. (2018). *Improved Design and Parametric Study of Controlled Jet Impingement Cooling System for Hot Steel Plates, Using Mechanistic Modeling.* Enugu: Post Graduate Studies, Enugu state university of science and technology.
10. Roy, J. I. (2011). Heat Transfer Performance of an Oil jet Impingement on a Downward Facing Stainless Steel Plate. *International Journal of Thermal Science, II*(15).
11. Shankar, R. S. (2019). Unsteady Heat Transfer: Lumped Thermal Capacity Model. clarkson university.